AR-NE5C, AR-NE7A, BL-18C/2018G023, 2018G503, 2020G073

In-situ X-ray diffraction study of phase transitions in ScOOH

Yoshiaki ITO[1], Osamu IKEDA[1], Rintaro BAN[1], Taito KUBOTA[1], Tatsuya SAKAMAKI[1], Takahiro KURIBAYASHI[1] and Akio SUZUKI[1,*]
[1] Tohoku University, Sendai 980-8578, Japan

1 Introduction

Both δ-AlOOH and ε-FeOOH, which exhibit an InOOH-type structure ($P2_1nm$, Z = 2) could carry water to the Earth's lower mantle. Hydrous minerals in subducting slabs transport water to the Earth's interior, and these two hydrous phases are stable under the conditions of the lower mantle. Various high-pressure phases of oxyhydroxides $M^{3+}OOH$ (M = Al, Sc, V, Cr, Mn, Fe, and Ga) exhibit a diaspore-type structure ($Pbnm$, Z = 4) under ambient conditions, and an InOOH-related structure under high pressures [1–3]. In recent years, high-pressure phase transitions of InOOH-type $M^{3+}OOH$ have been studied to improve our understanding of the water storage capacity under the high-pressure conditions of the interiors of super-Earth or ice giant exoplanets [4–7].

ScOOH has a diaspore-type structure (α-ScOOH) under ambient conditions and transforms into an InOOH-type structure at 8 GPa [8, 9]. YbOOH-type ScOOH ($P2_1/m$, Z = 2) was synthesized using hydrothermal techniques under pressures greater than 10 GPa and at a temperature of 400 ºC [10]. YbOOH-type structures have not been observed as a high-pressure structure in the other InOOH-type $M^{3+}OOH$ phases except for InOOH, which was predicted by DFT calculation [6] to adopt the YbOOH-type structure above 51 GPa. It is still unclear whether the stability fields of other structures exist or not, and in-situ X-ray diffraction (XRD) studies to observe the ScOOH phase transitions have not yet been conducted.

To determine the phase transition sequence and phase boundaries of ScOOH, we conducted in-situ XRD measurements on ScOOH up to 11 GPa and 900 K [11].

2 Experiment

In-situ XRD experiments were conducted at beamlines AR-NE5C and AR-NE7A of the Photon Factory at the High-Energy Accelerator Research Organization (KEK), Japan. A cubic-type multi-anvil apparatus, MAX80 [12], was used at AR-NE5C for high-pressure generation. An MA 6-6 type cell assembly [13] was used, containing six second-stage tungsten carbide (WC) anvils with a truncated edge length of 5.0 or 6.0 mm. The pressure medium was a mixture of amorphous boron and epoxy resin, with an edge length of 9.0 mm. High temperatures were generated by the resistive heating of a cylindrical graphite heater. For the experiments conducted at AR-NE7A, a 6-8 Kawai-type multi-anvil apparatus, MAX-III [14,15], was applied. We used WC cubes with an edge length of 22 mm and a truncated edge length of 5.0 mm. The cell assembly contained a ZrO_2 pressure medium, the amorphous boron and epoxy resin pressure medium, a cylindrical TiB_2-hBN (BN Composite EC, DENKA) heater, and molybdenum electrodes. The starting material was a mixture of powdered boehmite-type metastable γ-ScOOH (99.9% purity; Kojundo Chemical Laboratory Co., Ltd.) and NaCl (99.99% purity; Suprapur, Merck) with a 1:1 volume ratio, and the mixture was enclosed in the cell assembly. The pressure was determined according to the NaCl equation of state described by Brown [16], while the temperature was monitored using a W3%Re/W25%Re thermocouple. Energy-dispersive XRD was conducted, and the diffracted X-rays were collected using a germanium solid-state detector at a diffraction angle (2θ) of 6°. The samples were first compressed to the target press load at ambient temperature, and then heated to the target temperature. The phase transitions of samples were observed by time-resolved XRD measurements.

3 Results and Discussion

The representative time-resolved in-situ XRD patterns are shown in Figure 1 and Figure 2. Pressure-induced phase transitions between α-ScOOH and InOOH-type ScOOH and between InOOH-type ScOOH and YbOOH-type ScOOH were observed. The estimated phase boundaries among the three stable phases are shown in Figure 3. From the experimental results, the phase boundary between α-ScOOH and InOOH-type ScOOH is represented by a linear equation:

$$P(\mathrm{GPa}) = (0.0009 \pm 0.0015) \times [T(\mathrm{K}) - 700] + 4.33 \pm 0.04$$

The phase boundary between InOOH-type ScOOH and YbOOH-type ScOOH is also represented by a linear equation:

$$P(\mathrm{GPa}) = (-0.0029 \pm 0.0002) \times [T(\mathrm{K}) - 800] + 8.1 \pm 0.3$$

The experimental results showed that ScOOH exhibited the phase transition sequence (diaspore-type ($Pbnm$) → InOOH-type ($P2_1nm$) → YbOOH-type ($P\bar{4}2_1m$)). The same series of phase transitions has not been observed in the other $M^{3+}OOH$ phases.

Previous experimental studies have proposed two phase transitions of InOOH-type $M^{3+}OOH$ at high pressure. One is the transition of AlOOH to the orthorhombic *Pbca* AlOOH at 190 GPa [7], and the other is the transition of InOOH to pyrite-type InOOH at 14 GPa [4]. This study experimentally confirmed that phase transition from InOOH-type to YbOOH-type ScOOH occurs above 8.1 GPa.

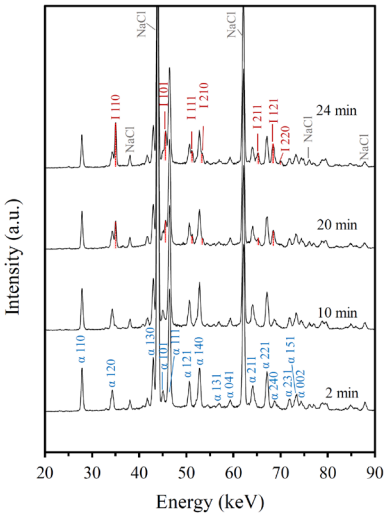

Fig. 1: Time-resolved X-ray diffraction patterns during phase transitions at 5.53 GPa and 650 K. Abbreviations of the peaks: α, α-ScOOH; I, InOOH-type ScOOH.

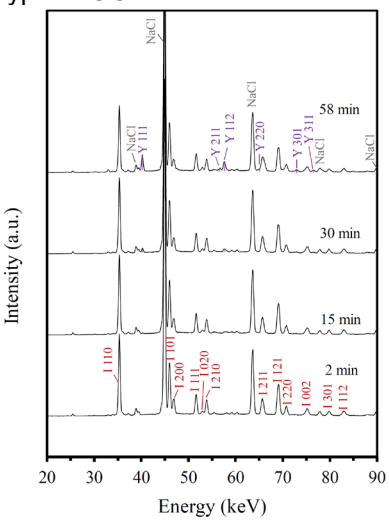

Fig. 2: Time-resolved X-ray diffraction patterns during phase transitions at 9.03 GPa and 750 K. Abbreviations of the peaks: I, InOOH-type ScOOH; Y, YbOOH-type ScOOH.

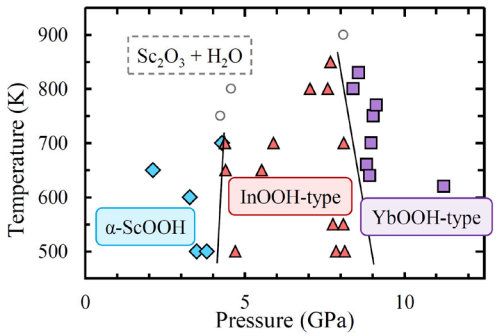

Fig. 3: Phase diagram of ScOOH. Meaning of the symbols: blue diamond, α-ScOOH; red triangle, InOOH-type ScOOH; purple square, YbOOH-type ScOOH; open circle, $Sc_2O_3 + H_2O$. The solid lines indicate the experimentally estimated phase boundaries.

Acknowledgement

This work was supported by the JSPS Japanese-German Graduate Externship and the JSPS KAKENHI Grant Numbers JP15H05828, JP19H01985, JP19K21890, JP17H04860, JP20H04604.

References

[1] A. Suzuki *et al.*, *Phys. Chem. Miner.* **27**, 689 (2000).
[2] J. Chenava *et al.*, *J. Solid State Chem.* **6**, 1 (1973).
[3] N.A. Nikolaev *et al.*, *J. Alloys Compd.* **459**, 95 (2008).
[4] A. Sano *et al.*, *J. Miner. Petrol. Sci.* **103**, 152 (2008).
[5] M. Nishi *et al.*, *Nature* **547**, 205 (2017).
[6] A.K. Verma *et al.*, *Am. Mineral.* **103**, 1906 (2018).
[7] M. Nishi *et al.*, *Icarus* **338**, 113539 (2020).
[8] A.N. Christensen and S.J. Jensen, *Acta Chem. Scand.* **21**, 121 (1967).
[9] A.N. Christensen, *Mater. Res. Bull.* **6**, 691 (1971).
[10] N.A. Bendeliani *et al.*, *High Temp-High Press.* **5**, 701 (1973).
[11] Y. Ito *et al.*, *High Press. Res.* (2021) DOI: 10.1080/08957959.2021.1964495
[12] O. Shimomura *et al.*, In: Minomura S, editor. Solid State Physics Under Pressure: Recent Advance with Anvil Devices, Tokyo, KTK Scientific Publishers, p. 351–356 (1985).
[13] N. Nishiyama *et al.*, *High Press. Res.* **28**, 307 (2008).
[14] N. Funamori *et al.*, *Special Issue Rev High Pressure Sci Technol.* **10**, 222 (2000).
[15] A. Suzuki *et al.*, *Phys. Chem. Miner.* **38**, 59 (2011).
[16] J.M. Brown, J. Appl. Phys. **86**, 5801 (1999).

* akio.suzuki.c5@tohoku.ac.jp